THE JOURNAL OF PHYSICAL CHEMISTRY B

ARTICLE

pubs.acs.org/JPCB

Epitaxial Crystallization of Poly(3-hexylthiophene) on a Highly Oriented Polyethylene Thin Film from Solution

Haixin Zhou, Shidong Jiang, and Shouke Yan*

State Key Laboratory of Chemical Resource Engineering, Beijing University of Chemical Technology, Beijing 100029, China

ABSTRACT: Crystallization of P3HT on highly oriented PE ultrathin films via solution-deposition has been studied by means of optical microscopy, atomic force microscopy, Fourier transform infrared spectroscopy (FTIR), and electron diffraction. The results clearly indicated the occurrence of heteroepitaxy of P3HT on the PE substrate, which results in a parallel alignment of P3HT on the PE substrate. FTIR spectra and electron diffraction analyses demonstrate that molecular chains of P3HT are oriented in the film plane and aligned parallel to the chain direction of PE substrate crystals, while the (100) lattice plane of P3HT is in contact with the PE substrate. The observed epitaxy can be explained in terms of an excellent one-dimensional lattice matching between the interchain distances of PE in the (110) lattice plane and P3HT in the (100) lattice plane. This kind of epitaxial crystallization provides an efficient way for fabricating large area P3HT films with unique oriented structures.

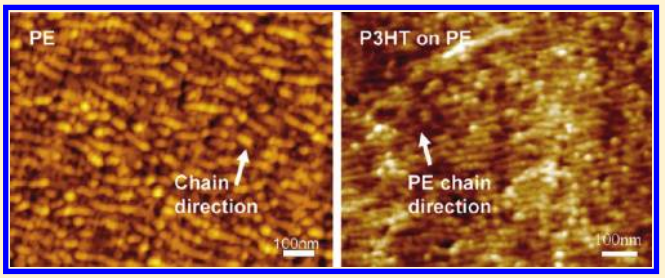

1. INTRODUCTION

Functional conjugated polymers have been widely investigated as active layers in optoelectronic devices during the past few years.[1−5] Among these conjugated polymers, regioregular poly(3-hexylthiophene) (P3HT) attracts the most attention because of its high field-effect mobility and solution-processability.[1,4,5] Enormous effort has been devoted to further improving its carrier mobility.[6−10] It was found that single-crystalline microwires of P3HT can provide well-resolved polymer electronic microdevices with high current sensing and low voltage-gate modulation. Moreover, the single crystal of P3HT has an anisotropic feature with the charge carrier transporting along the crystal growth direction, which results in the high mobility of electronic microdevices ($0.1-0.3\ cm^2\ V^{-1}\ s^{-1}$).[11,12] It should be pointed out that the P3HT thin films prepared via common methods, such as spin-coating, exhibit normally much poorer charge carrier mobility compared to that of the single crystals. Considering that preparation of single crystal with sufficient size is hardly possible for polymers, from a practical standpoint, it is of great significance for a better modification of structural anisotropy for large area P3HT film, so as to fabricate high performance electrical microdevices.

Epitaxy can control the crystal structure and orientation of the deposit materials, as is well demonstrated in the literature.[13−16] Therefore, numerous conjugated oligomers and polymers have been grown epitaxially on the surfaces of inorganic single crystals for fabricating photovoltaic and electroluminescent devices.[17−21] For P3HT, epitaxial crystallization of it on highly oriented pyrolitic graphite (HOPG) has been confirmed by various groups.[22,23] Also the directional solidification of it on 1,3,5-trichlorobenze has been reported by Brinkmann et al.[24,25] The epitaxial crystallization of P3HT on polymeric substrate has, however, not been reported up to date. Recently, using the highly oriented polyethylene (PE) as polymeric substrate, we have successfully grown the small molecular compound perylo[1,12-b,c,d]thiophene epitaxially from vapor phase, and an oriented thin film with the unique crystal structure of perylo[1,12-b,c,d]thiophene has been obtained.[26] It is expected that the oriented PE substrate may also be capable of inducing epitaxial crystallization of P3HT. This is, however, difficult to fulfill since the P3HT has a higher melting point than the PE, namely melt crystallization of P3HT on the oriented PE substrate is impossible. Moreover, the P3HT cannot be evaporated, which leads to the epitaxial crystallization of P3HT on the oriented PE substrate from vapor phase also impossible. Considering that spin-coating is a frequently used method to fabricate polymer thin films, we have therefore tested the epitaxial ability of P3HT on highly oriented PE films from solution during spin-coating in the present work. The results show that the P3HT can epitaxially grow on the PE substrate to produce large area well-ordered P3HT thin layers. The mutual epitaxial relationship between the P3HT and PE crystals was determined by FTIR spectroscopy and electron diffraction analyses.

2. EXPERIMENTAL SECTION

2.1. Materials. Regioregular P3HT with high molecular weight (M_w = 87 kDa) with head-to-tail regiospecific conformation more than 99% was purchased from Sigma-Aldrich. High-density polyethylene (PE), Lupolen 6021DX, was obtained from

Received: June 20, 2011
Revised: August 31, 2011
Published: October 18, 2011

ACS Publications © 2011 American Chemical Society

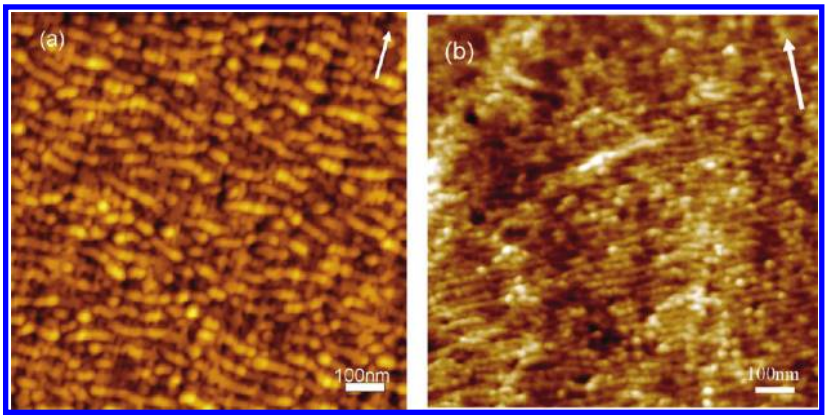

Figure 1. AFM height images of (a) an oriented PE film and (b) the morphology of P3HT grown on the PE substrate. The white arrows indicate the drawing directions of PE films during preparation.

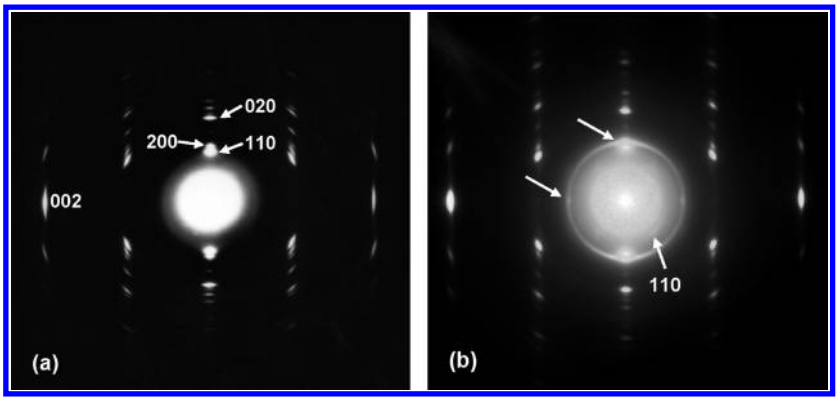

Figure 2. Electron diffraction patterns of the PE substrate film (a) and the P3HT-PE double-layered film (b) with the main reflections of P3HT as well as PE indexed.

BASF AG Ludwigshafen, Germany. The analytical pure chloroform used here was purchased from Beijing Chemical Works.

2.2. Preparation. A highly oriented thin film of PE was prepared according to a melt-draw technique introduced by Petermann and Gohil.[27] The original P3HT sample was dissolved in chloroform with concentrations of 0.1 and 0.5 wt % at 60 °C. Considering the thermochromism of P3HT, the solution was used immediately as it was prepared. The P3HT thin film was spin-coated on the oriented PE film from its solution at 2000 rpm for 30 s in air at room temperature. The thicknesses of the obtained highly oriented PE and P3HT thin films were determined from AFM height profiles by partially removing the sample films from the substrates and then evaluating the distance between the substrate surface and the average of all the heights measured through a linear scan across the sample surface. Height profiles recorded at different locations and/or with different directions on the sample surface show that the thicknesses of the samples prepared are basically uniform. The thicknesses of PE films range from 30 to 50 nm, whereas the thicknesses of P3HT thin films obtained from 0.1 and 0.5 wt % solution range from 10 to 30 nm and 60 to 80 nm, respectively. The thin P3HT films (spin-coated from 0.1 wt % solution) were used for AFM and TEM tests, and the thicker films (spin-coated from 0.5 wt % solution) were used for POM and FTIR tests.

2.3. Characterization. The optical microscopy images were obtained by using the Axioskop 40A Pol optical microscope (Carl Zeiss). The surface morphology of P3HT films on the PE substrates was studied by using an Agilent Technologies 5500 atomic force microscope (Agilent Technologies Co. Ltd., U.S.) at room temperature in air. The images were obtained by means of tapping mode (height and phase) with a silicon cantilever having a spring constant of 20−30 N/m and a resonating frequency of 320−350 kHz, and the scanning rates varied from 2 to 5 μm/s. For FTIR analysis, a Spectrum 100 FT-IR spectrometer (Perkin-Elmer) was used. The wavenumber of the infrared spectrum starts from 450 to 4000 cm^{-1}, and the polarized infrared was used in order to identify the chain directions of P3HT and PE. For transmission electron microscopy (TEM) examination, the P3HT/PE thin films were detached from the substrate glass slide with the help of poly(acrylic acid) (PAA) and mounted onto 400 mesh TEM copper grids without any further thermal treatment. TEM observations were performed using a JEOL JEM-2100 with an accelerating voltage of 200 kV.

3. RESULTS AND DISCUSSION

We present first the morphologies of the oriented PE substrate film in Figure 1a. The white arrow in the picture represents the drawing direction of the PE film during its preparation. From Figure 1a, we see that the PE substrate film consists of an oriented lamellar structure with the lamellae aligned preferentially perpendicular to the drawing direction during film preparation. The average thickness of the PE lamellae is about 20 nm. With close inspection, a shish-kebab morphology can be recognized from Figure 1a. Moreover, it seems that some of the PE microcrystallites exhibit different orientations. This may be caused by

different folding planes combined with different spatial arrangements of the PE crystals as reported in a previous paper.[28] When crystallizing the P3HT on the oriented PE substrate, see Figure 1b, oriented microcrystallites of P3HT were also observed. The P3HT crystals orient in a similar way as that of the PE substrate film, namely aligned preferentially perpendicular to the drawing direction of the PE substrate film. The preferred orientation of P3HT crystals grown on the oriented PE substrate suggests the occurrence of molecular epitaxy of P3HT on the PE substrate. It should be pointed out that (i) the P3HT lamellae are clearly thinner than the PE ones, which may be related to the relative lower crystallization temperature of P3HT during spin-coating (i.e., room temperature), and (ii) the P3HT microcrystallites exhibit a block- or pearl-like appearance, which resembles more or less the PE kebab structures shown in Figure 1a. This demonstrates the high nucleation ability of PE toward P3HT, which leads to the formation of abundant P3HT microcrystallites. These micrcrystallites align together resulting in the formation of pearl-like structures. Actually, the spin-coated P3HT thin films without further treatment also consist generally of short lamellar structures. Moreover, with close inspection, it seems that there are some P3HT microcrystallites with random orientation. This may be caused by the quick crystallization process of P3HT during spin-coating.

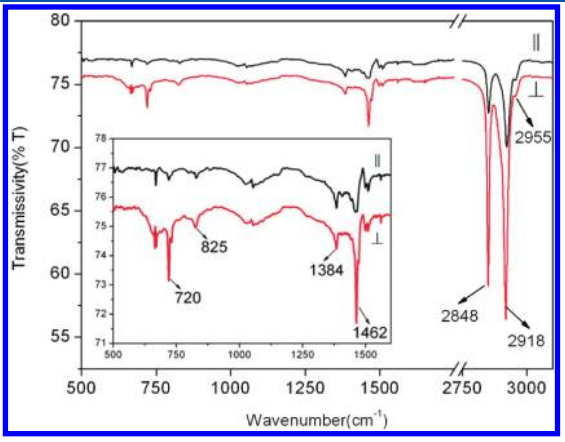

Figure 3. Polarized FTIR spectra of a P3HT/PE layered sample. The ⊥ and ∥ indicate that the electron vectors are perpendicular and parallel to the draw direction of PE, respectively. The inset presents the enlarged spectra in the region of 500−1600 cm^{-1}.

To disclose the epitaxial ability of P3HT on PE and their mutual orientation relationship, electron diffraction patterns were recorded. Figure 2a shows the electron diffraction pattern of the PE substrate film with the main reflections being indexed. All of the appeared PE reflection spots can be accounted for by the orthorhombic unit cells with axes a = 0.74, b = 0.494, and c = 0.2534 nm. The sharp and well-defined diffraction spots of PE crystals indicate the high orientation of the PE substrate. The coexistence of (110), (200), and (020) diffraction spots of PE demonstrates that the melt-drawn PE film exhibits a fiber orientation with molecular chains aligned in the drawing direction and the crystallographic a- and b-axes rotated randomly about the c-axis. The electron diffraction pattern of P3HT-PE double-layered film is presented in Figure 2b. It can be recognized that the reflections contributed by the P3HT crystals also show preferred orientation, which confirms the occurrence of heteroepitaxy between P3HT and PE. All of the observed P3HT diffractions can be accounted for by the orthorhombic unit cells with parameters a = 1.663, b = 0.775, and c = 0.777 nm.[29] The innermost reflection spots have been unambiguously indexed as the (011) diffractions of the P3HT crystals, as indicated in the picture. This implies that the epitaxial crystallization of P3HT on the PE substrate results in the (100) lattice plane of P3HT preferentially in contact with the PE substrate. Moreover, a Debye−Scherrer ring at the location of either (002) or (020) P3HT diffraction has been observed. This is in accordance with the AFM observation and indicates the existence of some random oriented P3HT crystals. Nevertheless, there exist diffraction maxima of P3HT crystals on the Debye−Scherrer ring between the $(110)_{PE}$ and $(200)_{PE}$ reflections and at the same lattice spacing along the (002) direction of the PE substrate crystals, as indicated by the white arrows. This indicates the preferred orientation of the P3HT grown on the oriented PE substrate, even though the orientation is not as good as that of the used PE substrates. This should originate from the fact that the crystallization of polymers is very fast during spin-coating. Furthermore, it should be pointed out that the above-mentioned diffraction maxima of P3HT can be indexed for either the (002) or the (020) diffraction. It is, however, hard to index them undoubtedly due to the almost same lattice distances of the (002) and (020) P3HT lattice planes. In other words, we cannot establish the chain orientation of P3HT on the PE substrate unambiguously through the obtained electron diffraction. To find out the exact mutual orientation of the heteroepitaxy

Table 1. Characteristic Infrared Bands of PE in Strong Absorbance Regions[a]

band (wavenumber)	assignments	transition motion direction	abbreviation
2918	asymmetric CH_2 stretching	⊥ to the C−C skeleton axis ⊥ to the C−C skeleton plane	$\nu_{as}(CH_2)$
2848	symmetric CH_2 stretching	⊥ to the C−C skeleton axis ∥ to the C−C skeleton plane	$\nu_s(CH_2)$
1467	CH_2 bending in amorphous phase	⊥ to the C−C skeleton axis	$\delta(CH_2)_{amorphous}$
1462	symmetric CH_2 bending in crystalline phase	⊥ to the C−C skeleton axis ∥ to the crystallographic b-axis	$\delta_s(CH_2)_{crystalline}$
731	CH_2 rocking in phase in crystalline phase	⊥ to the C−C skeleton axis ∥ to the crystallographic a-axis	$\gamma_{in}(CH_2)$
720	CH_2 rocking out of phase in crystalline	⊥ to the C−C skeleton axis ∥ to the crystallographic b-axis	$\gamma_{out}(CH_2)$

[a] The following abbreviations have been used: ν_{as} = asymmetric stretching, ν_s = symmetric stretching, δ_a = asymmetric deformation, δ_s = symmetric deformation, γ = rocking vibration.

dx.doi.org/10.1021/jp205755r |J. Phys. Chem. B 2011, 115, 13449–13454

between P3HT and PE, polarized FTIR was used to analysis the chain orientation of P3HT crystallized on the PE substrate.

Figure 3 shows the polarized FTIR spectra of a P3HT/PE layered sample. Differences between the FTIR spectra with the electron vectors perpendicular "⊥" and parallel "∥" to the draw direction of the PE thin film can be clearly recognized. For a better understanding of the obtained FTIR spectra, the assignments of the characteristic bands for both the PE and the P3HT should be discussed at first. The infrared spectroscopy study of PE has been extensively conducted and agreement on the band assignments has been achieved.[30−36] Table 1 summarizes the useful characteristic FTIR bands of PE in strong absorbance regions given in the literatures. On the other hand, the infrared spectroscopy investigation of P3HT has less been conducted.[37−45] Anyway, general assignments for the bands observed in the IR spectrum of P3HT were also given in some of the literatures, even though there is still no agreement between the results given by different authors. According to these literatures, the assignments of the P3HT IR absorption bands observed in our experiments are summarized in Table 2. From Tables 1 and 2, it is clear that the IR band at 2955 cm^{-1} can be attributed to the asymmetric stretching of the CH_3 groups in the P3HT, whereas the band at 1384 cm^{-1} is attributed to the deformation of the CH_3 groups in the P3HT. The bands at 2918 and 2848 cm^{-1} are mainly related to the PE substrate. There may also be the contribution of the P3HT since corresponding CH_2 vibrations of P3HT located at 2921 and 2852 cm^{-1} can be overlapped with the PE ones.[39] Also the bands near 1462 cm^{-1} could be contributed by both PE and P3HT related to the asymmetric and symmetric stretching vibrations of the CH_2 groups in PE as well as the asymmetric and symmetric stretching vibrations of the C═C units in P3HT. The band at 720 cm^{-1} is solely assigned to the PE substrate and the band at 825 cm^{-1} is related only to the P3HT. According to the above assignments, it can be observed from Figure 3 that the 2955 and 1384 cm^{-1} bands attributed to the side methyl groups show no difference when the electron vector perpendicular or parallel to the PE chain direction. However, the intensities of the bands at 2918, 2848, and 1462 cm^{-1} are tremendously increased when the electron vector perpendicular to the PE drawing direction. Since these bands exhibit perpendicular transition moments with respect to the main chain of PE, these features confirm that the chain direction of PE is aligned in the drawing direction, which is in good agreement with the electron diffraction results. It may also reflect a parallel chain alignment of P3HT with the PE substrate crystals since there may be also the contribution of P3HT. This is further confirmed by the intensity change of the band at 825 cm^{-1} (inset), which is assigned to the aromatic C−H out of plain deformation. As this band is suggested to exhibit a perpendicular transition moment with respect to the main chain of P3HT, the intensity increment of it when the electron vector perpendicular to the drawing direction of the PE indicates that the P3HT chains are preferentially aligned parallel to the chain direction of the substrate PE.

Table 2. Characteristic Infrared Bands of P3HT[a]

wavenumber(cm^{-1})	assignments
2955	$\nu_{as}(CH_3)$
2921	$\nu_{as}(CH_2)$
2852	$\nu_s(CH_3)$
1456	$\nu_s(C{=}C)$
1384	δ (CH_3)
825	δ $(C_\beta{-}H)$ in crystalline phase

[a] The following abbreviations have been used: ν_{as} = asymmetric stretching, ν_s = symmetric stretching, δ_a = asymmetric deformation, δ_s = symmetric deformation.

The above presented experimental results clearly indicate the occurrence of epitaxial crystallization of P3HT from solution on an oriented PE substrate with the chain directions of both polymers parallel. Now the aspects about its mechanism and feasibility for preparing large area oriented P3HT film should be commented. For the epitaxial mechanism, comparing the unit cell parameters of both polymers, excellent matching between the interchain distances of PE in the (110) plane with P3HT in the (100) plane (0.411 vs 0.416 nm) can be found. The mismatchings of ca. 1.2% is well below the upper limit (considered to be 15% by Wittmann and Lotz[46]) for the occurrence of polymer epitaxy.

To check the feasibility of epitaxial method for preparing large area oriented P3HT film, the as prepared P3HT-PE double-layered films were observed through optical microscope, which can provide the morphologies of the sample with hundreds of micrometers. For a direct comparison of the P3HT crystallized on the PE substrate and glass slide, a boundary region with the P3HT crystallized partially on PE and partially on the glass slide is shown in Figure 4a. The PE substrate is located at the lower left part of Figure 4a where its boundary line can be recognized. The arrow indicates the chain direction of highly oriented PE substrate crystals, which is parallel to the analyzer direction. It can be found that the birefringences are uniform within the P3HT-PE

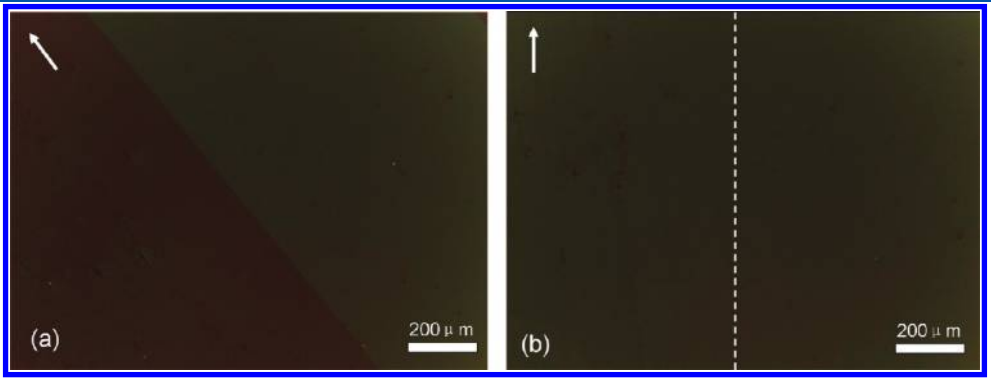

Figure 4. (a) Optical micrograph of a P3HT-PE double-layered sample taken in a boundary area with P3HT partially crystallized on the PE substrate (located at the lower left part of the picture with the arrow indicating its chain direction) and partially on the glass slide. (b) The optical micrograph taken from the same area as shown in part (a) but rotated for 45° clockwise about the light beam. The dash line illustrates the boundary of PE substrate.

double layers and the P3HT single layer, respectively. This indicates the formation of a homogeneous structure of the P3HT on PE substrate, as compared with the P3HT spin-coated on the neat glass slide. The weak birefringence of the P3HT/PE double layers implies the extinction of the sample under this condition. In other words, it indicates an oriented structure of P3HT crystallized on the PE substrate. According to the role of light extinction under polarized optical microscope, the optical microscopy result helps to confirm the chain parallel epitaxy between P3HT and PE. This has been further tested by sample rotation. As illustrated in Figure 4b, when the sample was rotated 45° clockwise about the light beam axis, the birefringence of the sample within the P3HT-PE double-layered area increased remarkably, whereas the birefringence of the P3HT spin-coated on glass slide remains in principle unchanged, demonstrating the occurrence of exceptional extinction when the chain axis of PE is parallel to the analyzer (Figure 4a). Moreover, the birefringence of P3HT/PE double layers in Figure 4b is only slightly stronger than that of P3HT on the glass slide. This indicates that birefringence of the sample is mainly from the P3HT crystals. Otherwise, a much stronger birefringence should be observed for the double-layered sample. According to the above discussion, these optical microscopy results demonstrate that large area ordered P3HT thin films with a uniformly oriented structure can be prepared through epitaxial crystallization from solution on the oriented PE substrate.

4. CONCLUSION

In summary, the crystallization of P3HT on a highly oriented PE substrate from solution during the spin-coating process has been studied. The AFM results clearly indicate that the P3HT crystallizes epitaxially on an oriented PE substrate, leading to the formation of parallel aligned microcrystallites, i.e., the occurrence of heteroepitaxy. Electron diffraction results confirm the occurrence of heteroepitaxy and demonstrate that the (100) lattice plane of P3HT is in contact with the highly oriented PE substrate. However, becasue of the close lattice spacing of the (002) and (020) P3HT lattice planes, the exact chain orientation of the P3HT on the PE substrate cannot be judged only by the electron diffraction. Polarized FTIR analysis illustrates that the epitaxy of P3HT on the PE substrate leads to a parallel alignment of P3HT molecules with their chain direction preferentially along the PE chain direction. All of these indicate that the PE exhibits strong nucleation ability toward P3HT, which results in the crystallization of P3HT on the PE substrate with preferred crystallographic orientations even in a very fast crystallization process during the spin-coating. This results from the close matching between the interchain distance of PE in the (110) lattice plane and that of P3HT in the (100) lattice plane. Optical microscopy observation demonstrates that a large area ordered P3HT thin film with uniform oriented structure can be prepared through epitaxial crystallization from solution.

AUTHOR INFORMATION

Corresponding Author

*E-mail: skyan@mail.buct.edu.cn. Tel: + 86-10-64455928. Fax: + 86-10-64455928.

ACKNOWLEDGMENT

Financial support of the National Natural Science Foundations of China (No. 50833006, 20634050 and 50973008) and the program of Introducing Talents of Discipline to Universities (B08003) is gratefully acknowledged.

REFERENCES

(1) Sirringhaus, H.; Brown, P. J.; Friend, R. H.; Nielsen, M. M.; Bechgaard, K.; Langeveld-Voss, B. M. W.; Spiering, A. J. H.; Janssen, R. A. J.; Meijer, E. W.; Herwig, P.; de Leeuw, D. M. *Nature* **1999**, *401*, 685–688.

(2) Dimitrakopoulos, C. D.; Mascaro, D. J. *IBM J. Res. Dev.* **2001**, *45*, 11–27.

(3) Fix, W.; Ullmann, A.; Ficker, J.; Clemens, W. *Appl. Phys. Lett.* **2002**, *81*, 1735–1737.

(4) Kim, D. H.; Han, J. T.; Park, Y. D.; Jang, Y.; Cho, J. H.; Hwang, M.; Cho, K. *Adv. Mater.* **2006**, *18*, 719–723.

(5) Joshi, S.; Grigorian, S.; Pietsch, U.; Pingel, P.; Zen, A.; Neher, D.; Scherf, U. *Macromolecules* **2008**, *41*, 6800–6808.

(6) Zen, A.; Pflaum, J.; Hirschmann, S.; Zhuang, W.; Jaiser, F.; Asawapirom, U.; Rabe, J. P.; Scherf, U.; Neher, D. *Adv. Funct. Mater.* **2004**, *14*, 757–764.

(7) Zen, A.; Saphiannikova, M.; Neher, D.; Grenzer, J.; Grigorian, S.; Pietsch, U.; Asawapirom, U.; Janietz, S.; Scherf, U.; Lieberwirth, I.; Wegner, G. *Macromolecules* **2006**, *39*, 2162–2171.

(8) Chang, J. F.; Sun, B.; Breiby, D. W.; Nielsen, M. M.; Sölling, T. I.; Giles, M.; McCulloch, I.; Sirringhaus, H. *Chem. Mater.* **2004**, *16*, 4772–4776.

(9) Yang, H.; Shin, T. J.; Yang, L.; Cho, K.; Ryu, C. Y.; Bao, Z. *Adv. Funct. Mater.* **2005**, *15*, 671–676.

(10) Ho, P. K. H.; Chua, L.-L.; Dipankar, M.; Gao, X. Y.; Qi, D. C.; Wee, A. T. S.; Chang, J. F.; Friend, R. H. *Adv. Mater.* **2007**, *19*, 215–221.

(11) Bao, Z.; Dodabalapur, A.; Lovinger, A. J. *Appl. Phys. Lett.* **1996**, *69*, 4108–4110.

(12) Sirringhaus, H.; Tessler, N.; Friend, R. H. *Science* **1998**, *280*, 1741–1744.

(13) Kopp, S.; Wittmann, J. C.; Lotz, B. *Polymer* **1994**, *35*, 916–924.

(14) Lovinger, A. J. *Polymer* **1981**, *22*, 412–413.

(15) Kopp, S.; Wittmann, J. C.; Lotz, B. *Polymer* **1994**, *35*, 908–915.

(16) An, Y. K.; Jiang, S. D.; Yan, S. K.; Sun, J. R.; Chen, X. S. *Chin. J. Polym. Sci.* **2011**, *29*, 513–519.

(17) Thayer, G. E.; Sadowski, J. T.; Meyer, zu; Heringdorf, F.; Sakurai, T.; Tromp, R. M. *Phys. Rev. Lett.* **2005**, *95*, 256106–1−4.

(18) Kiyomura, T.; Nemoto, T.; Yoshida, K.; Minari, T.; Kurata, H.; Isoda, S. *Thin Solid Film* **2006**, *515*, 810–813.

(19) Söhnchen, S.; Lukas, S.; Witte, G. J. *Chem. Phys.* **2004**, *121*, 525–534.

(20) Lukas, S.; Söhnchen, S.; Witte, G.; Wöll, C. *Chem. Phys. Chem.* **2004**, *5*, 266–270.

(21) Sadowski, J. T.; Nagao, T.; Yaginuma, S.; Fujikawa, Y.; Al-Mahboob, A.; Nakajima, K.; Sakurai, T.; Thayerb, G. E.; Tromp, R. M. *Appl. Phys. Lett.* **2005**, *86*, 073109–1−3.

(22) Grévin, B.; Rannou, P.; Payerne, R.; Pron, A.; Travers, J. P. *Adv. Mater.* **2003**, *15*, 881–884.

(23) Mena-Osteriz, E. *Adv. Mater.* **2002**, *14*, 609–616.

(24) Brinkmann, M.; Wittmann, J. C. *Adv. Mater.* **2006**, *18*, 860–863.

(25) Brinkmann, M.; Rannou, P. *Adv. Funct. Mater.* **2007**, *17*, 101–108.

(26) Jiang, S. D.; Qian, H. L.; Liu, W.; Wang, C. R.; Wang, Z. H.; Yan, S. K.; Zhu, D. B. *Macromolecules* **2009**, *42*, 9321–9324.

(27) Peterman, J.; Gohil, R. M. J. *Mater. Sci.* **1979**, *14*, 2260–2263.

(28) Chang, H.; Guo, Q.; Shen, D.; Li, L.; Qiu, Z.; Wang, F.; Yan, S. *J. Phys. Chem. B* **2010**, *114*, 13104–13109.

(29) Tashiro, K.; Kobayashi, M. *Polymer* **1997**, *38*, 2867–2879.

(30) Abbate, S.; Gussoni, M.; Zerbi, G. *J. Chem. Phys.* **1979**, *70*, 3577–3585.

(31) Agosti, E.; Zerbi, G.; Ward, I. M. *Polymer* **1992**, *33*, 4219–4229.

(32) Singhal, A.; Fina, L. J. *Polymer* **1996**, *37*, 2335–2343.

(33) Nielsen, J. R.; Woollett, A. H. *J. Chem. Phys.* **1957**, *26*, 1391–1400.

(34) Nielsen, J. R.; Holland, R. F. *J. Mol. Spectrosc.* **1961**, *6*, 394–418.
(35) Synder, R. G. *J. Mol. Spectrosc.* **1961**, *7*, 116–144.
(36) Tobin, M. C.; Carrano, M. J. *J. Chem. Phys.* **1956**, *25*, 1044–1052.
(37) Chen, T. A.; Wu, X. M.; Rieke, R. D. *J. Am. Chem. Soc.* **1995**, *117*, 233–244.
(38) Curtis, M. D.; Nanos, J. I.; Moon, H.; Jahng, W. S. *J. Am. Chem. Soc.* **2007**, *129*, 15072–15084.
(39) Singh, R. K.; Kumar, J.; Singh, R.; Kant, R.; Chand, S.; Kumar, V. *Mater. Chem. Phys.* **2007**, *104*, 390–396.
(40) Bolognesi, A.; Porzio, W.; Provasoli, F. *Makromol. Chem.* **1993**, *194*, 817–827.
(41) Winokur, M. J.; Spiegel, D.; Kim, Y.; Hotta, S.; Heeger, A. J. *Synth. Met.* **1989**, *28*, 419–426.
(42) Qiao, X. Y.; Wang, X. H.; Mo, Z. S. *Synth. Met.* **2001**, *118*, 89–95.
(43) Zerbi, G.; Chierichetti, B. *J. Chem. Phys.* **1991**, *94*, 4646–4658.
(44) Hsu, W. P.; Levon, K.; Ho, K. S.; Myerson, A. S.; Kwei, T. K. *Macromolecules* **1993**, *26*, 1318–1323.
(45) Yazawa, K.; Inoue, Y.; Yamamoto, T.; Asakawa, N. *J. Phy. Chem. B* **2008**, *112*, 11580–11585.
(46) Wittmann, J. C.; Lotz, B. *Prog. Polym. Sci.* **1990**, *15*, 909–948.